Spatial estimates of juvenile Pacific salmon (Oncorhynchus spp.) abundance in the Strait of Georgia

Patrick L. Thompson and Chrys M. Neville

Fisheries and Oceans Canada
Science Branch, Pacific Region
Pacific Science Enterprise Centre
West Vancouver, British Columbia
V7V 1H2

2024

Canadian Technical Report of
Fisheries and Aquatic Sciences 3597

Fisheries and Oceans Canada | Pêches et Océans Canada

Canada

Canadian Technical Report of Fisheries and Aquatic Sciences

Technical reports contain scientific and technical information that contributes to existing knowledge but which is not normally appropriate for primary literature. Technical reports are directed primarily toward a worldwide audience and have an international distribution. No restriction is placed on subject matter and the series reflects the broad interests and policies of Fisheries and Oceans Canada, namely, fisheries and aquatic sciences.

Technical reports may be cited as full publications. The correct citation appears above the abstract of each report. Each report is abstracted in the data base *Aquatic Sciences and Fisheries Abstracts*.

Technical reports are produced regionally but are numbered nationally. Requests for individual reports will be filled by the issuing establishment listed on the front cover and title page.

Numbers 1-456 in this series were issued as Technical Reports of the Fisheries Research Board of Canada. Numbers 457-714 were issued as Department of the Environment, Fisheries and Marine Service, Research and Development Directorate Technical Reports. Numbers 715-924 were issued as Department of Fisheries and Environment, Fisheries and Marine Service Technical Reports. The current series name was changed with report number 925.

Rapport technique canadien des sciences halieutiques et aquatiques

Les rapports techniques contiennent des renseignements scientifiques et techniques qui constituent une contribution aux connaissances actuelles, mais qui ne sont pas normalement appropriés pour la publication dans un journal scientifique. Les rapports techniques sont destinés essentiellement à un public international et ils sont distribués à cet échelon. II n'y a aucune restriction quant au sujet; de fait, la série reflète la vaste gamme des intérêts et des politiques de Pêches et Océans Canada, c'est-à-dire les sciences halieutiques et aquatiques.

Les rapports techniques peuvent être cités comme des publications à part entière. Le titre exact figure au-dessus du résumé de chaque rapport. Les rapports techniques sont résumés dans la base de données *Résumés des sciences aquatiques et halieutiques.*

Les rapports techniques sont produits à l'échelon régional, mais numérotés à l'échelon national. Les demandes de rapports seront satisfaites par l'établissement auteur dont le nom figure sur la couverture et la page du titre.

Les numéros 1 à 456 de cette série ont été publiés à titre de Rapports techniques de l'Office des recherches sur les pêcheries du Canada. Les numéros 457 à 714 sont parus à titre de Rapports techniques de la Direction générale de la recherche et du développement, Service des pêches et de la mer, ministère de l'Environnement. Les numéros 715 à 924 ont été publiés à titre de Rapports techniques du Service des pêches et de la mer, ministère des Pêches et de l'Environnement. Le nom actuel de la série a été établi lors de la parution du numéro 925.

Canadian Technical Report of
Fisheries and Aquatic Sciences 3597

2024

SPATIAL ESTIMATES OF JUVENILE PACIFIC SALMON (*ONCORHYNCHUS* SPP.) ABUNDANCE IN THE STRAIT OF GEORGIA

by

Patrick L. Thompson[1] and Chrys M. Neville[2]

[1]Pacific Science Enterprise Centre
Fisheries and Oceans Canada, 4160 Marine Dr.
West Vancouver, British Columbia, V7V 1H2, Canada

[2]Pacific Biological Station
Fisheries and Oceans Canada, 3190 Hammond Bay Road
Nanaimo, British Columbia, V9T 6N7, Canada

Cat. No. Fs97-6/3597E-PDF ISBN 978-0-660-70849-2 ISSN 1488-5379

Correct citation for this publication:

Thompson, P.L. and Neville, C.M. 2024. Spatial estimates of juvenile Pacific salmon (*Oncorhynchus* spp.) abundance in the Strait of Georgia. Can. Tech. Rep. Fish. Aquat. Sci. 3597: v + 30 p.

CONTENTS

ABSTRACT

Thompson, P.L. and Neville, C.M. 2024. Spatial estimates of juvenile Pacific salmon (*Oncorhynchus* spp.) abundance in the Strait of Georgia. Can. Tech. Rep. Fish. Aquat. Sci. 3597: v + 30 p.

We provide spatial estimates of the distribution of juvenile fish in the Strait of Georgia for all five species of Pacific salmon. These estimates were generated using a spatiotemporal generalized linear model and are based on standardized fishery-independent survey data from the Strait of Georgia juvenile Pacific salmon pelagic trawl survey from 2010 to 2020. We provide predicted catch per unit effort (CPUE), year-to-year variation in CPUE, and prediction uncertainty, for both summer (June–July) and fall (September–October) at a 0.5 km resolution, covering the majority of the strait. These results show that the surface 75 m of the entire Strait of Georgia is habitat for juvenile Pacific salmon from June through early October, but that distributions within the strait differ across species and between the early summer and fall. While there is interannual variability in abundances and distributions, our analysis identifies areas that have consistently high abundances across years. Results illustrate juvenile habitat use in the Strait of Georgia for the five species of Pacific salmon and can support ongoing marine spatial planning initiatives in the Pacific Region of Canada.

RÉSUMÉ

Thompson, P.L. and Neville, C.M. 2024. Spatial estimates of juvenile Pacific salmon (*Oncorhynchus* spp.) abundance in the Strait of Georgia. Can. Tech. Rep. Fish. Aquat. Sci. 3597: v + 30 p.

Nous fournissons des estimations spatiales de la répartition des poissons juvéniles dans le détroit de Georgia pour les cinq espèces de saumon du Pacifique. Ces estimations ont été générées à l'aide d'un modèle linéaire généralisé spatiotemporel et sont fondées sur les données des relevés normalisés indépendants de la pêche visant les saumons du Pacifique juvéniles dans le détroit de Georgia, qui ont été menés par chalut pélagique de 2010 à 2020. Nous fournissons les prévisions des captures par unité d'effort (CPUE), la variation annuelle des CPUE et l'incertitude des prévisions pour l'été (juin et juillet) et l'automne (septembre et octobre) à une résolution de 0,5 km; ces prévisions couvrent la majeure partie du détroit. Les résultats démontrent que dans tout le détroit de Georgia, la couche de 75 m sous la surface constitue un habitat pour les saumons du Pacifique juvéniles de juin au début d'octobre, mais que les répartitions dans le détroit diffèrent d'une espèce à l'autre et entre le début de l'été et l'automne. Bien qu'il y ait une variabilité interannuelle dans les abondances et les répartitions, notre analyse définit les zones où les abondances sont constamment élevées au fil des ans. Les résultats illustrent l'utilisation de l'habitat des juvéniles dans le détroit de Georgia pour les cinq espèces de saumon du Pacifique et peuvent appuyer les initiatives de planification spatiale marine en cours dans la région du Pacifique du Canada.

1 Introduction

Spatial information for juvenile Pacific salmon habitat in the Strait of Georgia bioregion is needed to support ongoing marine spatial planning initiatives. Marine spatial planning is a "public process of analyzing and allocating the spatial and temporal distribution of human activities in marine areas to achieve ecological, economic, and social objectives" (Ehler and Douvere 2009). Marine spatial planning is being advanced in five planning areas across Canada, including southern British Columbia (BC), and the Strait of Georgia comprises one of two bioregions in this planning area. As a key component of marine spatial planning in Canada, the Department of Fisheries and Oceans Canada (DFO) is developing the Canada Marine Planning Atlas, which provides decision makers with an overview of activities, ecological processes and relevant features in the various regions. Providing spatial data for the atlas is one of the key deliverables for DFO Science branch and a priority is to fill gaps in spatial data on species and habitat use, which includes Pacific salmon. Such information has been provided in the Strait of Georgia for species groups such as groundfish, eelgrass, invertebrates, marine mammals (new and updated datasets summarized in Robb et al. in prep). However, spatial information on juvenile Pacific salmon is a current data gap, and was not available for spatial planning initiatives that have been undertaken to date in other regions of BC (e.g., PNCIMA 2017; Diggon et al. 2022).

Fisheries and Oceans Canada has been conducting pelagic trawl surveys of juvenile Pacific salmon in the surface 75 m of the Strait of Georgia since 1998 (Beamish et al. 2000; Sweeting et al. 2003; Neville et al. 2023). These surveys, conducted in the early summer and fall, were initially designed to examine the early marine distribution, abundance and condition of juvenile Coho Salmon and Chinook Salmon. However, since the initiation of the surveys, all species of juvenile Pacific salmon as well as other species utilizing the surface waters of the strait have been sampled. One output of the surveys has been annual indices of juvenile abundance for all five species of Pacific salmon (Neville 2023). Due to the good spatial coverage of the surveys, the repeated nature of the surveys across both years and seasons, and the use of standard fisheries independent scientific protocols, these surveys are well suited for developing model-based spatially explicit estimates of juvenile Pacific salmon abundance across the Strait of Georgia bioregion. Assessments of the spatial variability of juvenile Pacific salmon abundance has been completed by examining catch per unit effort by set in the surveys and interannual changes (Neville unpublished). However, full model-based estimates that account for uncertainty in the observations and which can provide continuous predictions across the region are not currently available.

Geostatistical models are increasingly used to estimate the spatial distributions of species, including marine fish, and how those distributions are changing through time (e.g., Thorson et al. 2015; Anderson et al. 2019; Currie et al. 2019; Ovaskainen and Abrego 2020). These models account for the fact that observations of species' abundance that are in close proximity tend to be more similar than observations that are further apart (Anderson et al. 2021). Although the reason for spatial autocorrelation in species' abundances is generally due to ecological processes such as environmental responses, food web interactions, and movement (Thompson et al. 2020), data that captures these processes is often lacking. In these cases, geostatistical models can account for spatial autocorrelation that is present in the data through spatial and spatiotemporal random fields (Cressie and Wikle 2011). While this approach cannot directly assess which processes are responsible for the spatial patterns in species abundances, it offers the ability to estimate the spatial and temporal trends in the data. This allows these models to

make predictions across continuous space, including in locations that were not directly sampled, and where environmental data that could inform those predictions may be lacking (Anderson et al. 2021). Thus, geostatistical models offer an effective way of generating predictions of how species abundances vary across space and time that can be used to inform marine spatial planning and other management decisions.

Here we provide spatial estimates of juvenile abundance for all five species of Pacific salmon in the Strait of Georgia for summer (June–July) and fall (September–October) using geostatistical models based on data from the DFO Strait of Georgia juvenile salmon survey (Salmon Marine Interactions Program) in the years from 2010 to 2020. Continuous estimates are provided at a 0.5 km resolution throughout the Strait of Georgia. These estimates consist of: 1) mean catch per unit effort (CPUE), 2) year-to-year coefficient of variation (CV) of CPUE as a measure of the temporal variability, 3) binned biscale measures of mean vs. CV of CPUE to distinguish areas where abundance is consistently high vs. areas where it is high on average, but with high year-to-year variability, and 4) mean standard error in CPUE as a measure of uncertainty. Together this analysis provides a set of spatial estimates of juvenile Pacific salmon abundance in the Strait of Georgia bioregion that can support ongoing marine spatial planning initiatives as well as other management initiatives that require information about the spatial and temporal distribution of juvenile Pacific salmon in the region.

2 Methods

2.1 Strait of Georgia juvenile salmon survey

Surveys for juvenile Pacific salmon are conducted twice per year, once in summer (June–July) and once in fall (September–October). The trawl survey samples both near shore and offshore regions of the Strait of Georgia from Quadra Island in the north to the Canada–United States border in the south. The survey fishes a standard track line as described in Neville et al. (2023). The number of sets varies across seasons and years but range between 53 and 89 per survey. Sets are conducted during daylight hours (between 6 a.m. to 6 p.m. in summer and between 7 a.m. and 7 p.m. in fall), and typically last 30 min with the net towed at a speed of 4.5–5.0 knots. The net opening varies between sets depending on depth, vessel speed, and currents. However, on average, the opening is 13 m deep and 26 m wide (Neville 2023). The sets are conducted at different headrope depths (0, 15, 30,45, 60 m) following the protocols outlined in Beamish et al. (2000) and Sweeting et al. (2003). The depth strata are randomized each day with the greatest effort at the surface and declining effort at depth. This randomized design has remained consistent across all years of the surveys and for the standard track line sets provided in this document. All fish in each set are identified to species and enumerated. In addition to this standard track line, fishing occurs in adjacent areas, but these non-standard sets have been excluded from this analysis due to variability in areas fished in each survey, effort, and fishing protocols.

This analysis is based on surveys conducted between 2010 and 2020. We only included sets that lasted between 12 and 50 min and were conducted at depths less than or equal to 60 m (headrope depth). This dataset consisted of 1,588 sets (Figure 1). Of these sets, 83% were 30 min in duration, 12% were 20 min in duration and 1% were 15 min in duration. Based on average headrope tow depth, 43% were at the surface, 29% were at 15 m, 17% were at 30 m, 7% were at 45 m, 4% were at 60 m. Our analysis included all five species of Pacific salmon. For

Pink Salmon, only even-year surveys were included as this species has a two-year life cycle and are effectively absent from the Strait of Georgia in odd numbered years.

2.2 Geostatistical model of salmon abundance

We estimated the spatial distribution and abundance of each species of Pacific salmon using geostatistical models fit with sdmTMB (Anderson et al. 2022). For each species, we modelled the number of individuals caught in a set $Y_{s,t}$ at location s and time t using a negative binomial observation model (NB2 parameterization; Hilbe 2011) with a log link:

$$\begin{aligned} Y_{s\,t} &= log(\mu_{s\,t}) \\ \mu_{s\,t} &= \mathbf{X}_{s\,t}\boldsymbol{\beta} + \omega_s + \epsilon_{s\,t} \\ \omega &\sim \text{MVNormal}(0\ \Sigma_\omega) \\ \epsilon_{s\,t} &\sim \text{MVNormal}(0\ \Sigma_\epsilon) \end{aligned}$$

where $\mu_{s,t}$ represents the mean number of individuals caught estimated at location s and time t. The symbol $\mathbf{X}_{s,t}$ represents a vector of covariates (described below) that correspond to location s and time t and $\boldsymbol{\beta}$ represents a vector of fixed-effect coefficients. The parameters ω_s and $\epsilon_{s,t}$ represent spatial and spatiotemporal random effects, respectively. These random effects were assumed to be drawn from Gaussian Markov random fields with covariance matrices Σ_ω and Σ_ϵ that were constrained by Matérn covariance functions (Cressie and Wikle 2011). Location s was defined as the spatial coordinates at the mid point of each set. Each survey was assumed to be a single time unit t (e.g., fall 2012) for the purposes of the spatiotemporal random fields, and we assume that the spatiotemporal random fields are independent across time steps. The spatial random fields were modelled using a predictive process approach with a triangulated mesh (Lindgren and Rue 2015) and bilinear interpolation between vertices. We constructed the spatial mesh such that vertices had a minimum gap of 5 km. We also applied a coastline physical barrier, assuming that the spatial range over land is 0.2 of that over water (Bakka et al. 2019). smdTMB fits the model by maximum marginal likelihood using a mesh constructed in INLA (Rue et al. 2009; Lindgren et al. 2011; Lindgren and Rue 2015), a model template coded in TMB (Kristensen et al. 2016), the marginal likelihood function maximized with nlminb (Gay 1990), and the random effects integrated over via the Laplace approximation (Kristensen et al. 2016).

2.3 Model covariates

Model covariates were tow duration, mean tow depth, year as a factor, and Julian day. Tow duration, expressed as log hours, was modelled as an offset to account for the fact that longer tows are likely to catch more fish. Mean tow depth, representing the average depth in the water column for the tow, and was modelled using a penalized spline with three basis function dimensions, allowing for the number of fish caught to vary non-linearly with tow depth. Year was modelled as a factor to account for non-linear year-to-year variation in average fish abundance. Julian day was modelled as a penalized spline with four basis function dimensions, to account for non-linear variation in abundance across the year. This allowed us to account for the effect of year-to-year variation in the dates of the surveys on catch. We included tow duration, mean tow depth, and year in all models. Additionally, we included Julian day in the model if it increased the predictive power of the model as measured using cross validation (see below). This was the case for all species other than Chum Salmon. All model covariates other than tow duration were scaled to have a mean of 0 and a standard deviation of 1 prior to model fitting.

In exploratory analyses, we also considered including temperature, salinity, and zooplankton biomass from the SalishSeaCast model (Olson et al. 2020). We used mean values for each of these variables at the location, year and depth of the sets, for the month preceding the surveys. That is, May for the summer surveys and August for the fall surveys. However, based on the results of the exploratory analyses, we did not include the covariates from the SalishSeaCast model in our final models because they did not increase predictive accuracy as assessed by the temporal block cross validation procedure.

2.4 Model assessment

We compared the predictive accuracy of models with different structure using expected log pointwise density (Vehtari et al. 2017) using cross validation. This cross-validation procedure consisted of running the model multiple times using 5 folds and assessing how well the model could predict the held out data. Our final models were then fit using the full dataset. For our selected models, we assessed model fit by visual inspection of the residuals (Figure A.1) calculated using the DHARMa package (Hartig 2022).

2.5 Predictions

Predictions were made for each survey season (i.e., summer and fall) in each year from 2010 and 2020 over a 500 m by 500 m grid based on a 3 km buffer around the outer concave hull of the trawl coordinates (Figure 1). The concave hull was calculated using the 'sf_concave_hull' function from the sf package (Pebesma 2018) using a concavity ratio of 0.3 and excluding holes. Predictions were made as CPUE (catch per 60 min) for tows conducted in the surface waters (i.e., headrope at 0 m). For models that included Julian day, we used 182 (July 1) for the summer survey and 265 (September 22) for the fall survey, which were the median days for each of the surveys across all years.

Predictions were estimated as the mean CPUE (i.e., catch per 60 min) and the standard error for each grid cell in each survey period and year. The standard error was estimated as the standard deviation of 500 simulation draws from the joint precision matrix (Anderson et al. 2022). Mean CPUE and temporal variation in CPUE were estimated for each grid cell in each survey period by calculating the mean and CV (standard deviation divided by the mean) across all years in the dataset.

2.6 Code availability

All scripts used to generate these models are available at https://gitlab.com/dfo-msea/sog_juvenile_salmon_report.

3 Results

Overall, at least one species of juvenile Pacific salmon was caught in 94.8% of survey sets and 97.6% of survey sets targeting 0 and 15 m depths. Most (79.8%) sets caught at least two species and 12.8% of sets caught all five species.

3.1 Chinook Salmon

Our model estimates that juvenile Chinook Salmon are present across the full range of depths sampled in the survey, but CPUE decreases with depth (Figure A.2a). Juvenile Chinook Salmon were caught in 84.8% of sets. A total of 30,181 individuals was caught across all surveys, which equals 16.9% of all individuals caught across all Pacific salmon species. In summer, juvenile Chinook Salmon were predicted to be abundant but with low year-to-year variation on the northeastern margin of the Strait of Georgia from the Sunshine Coast to Desolation Sound and in the southern part of the region, near the Southern Gulf Islands (Figure 2a-c). Fall abundances are predicted to be highest in the southwestern part of the region (around the mouth of the Fraser river and the Southern Gulf Islands), but the temporal coefficient of variation is estimated to be higher in the fall compared to the summer, indicating that the areas of high juvenile Chinook Salmon abundance in fall vary from year-to-year. The standard error of the predictions, which represents uncertainty in the predictions, is relatively consistent across the region, but is higher in between Texada and Lasqueti Islands and on the northern end of the strait, near Desolation Sound (Figure 2d), corresponding to areas where the survey does not fish, or fishes less often and so model extrapolation is required (Figure 1).

3.2 Chum Salmon

Our model estimates that Juvenile Chum Salmon are present only in the surface 30 m (headrope depth 0 and 15 m; Figure A.2b). Juvenile Chum Salmon were caught in 66.1% of sets in this depth range. A total of 55,802 individuals was caught across all surveys, which equals 31.3% of all individuals caught across all species. In summer, juvenile Chum Salmon are predicted to follow a gradient from high abundance in the northwest between Texada and Quadra Islands to low abundance in the southeast near the Fraser River outflow (Figure 3a). In fall, juvenile Chum Salmon are predicted to be more evenly distributed across the region, with the highest abundance in the central and southern part of the strait (Figure 3a). The highest summer year-to-year coefficient of variation is estimated to be in the low abundance regions, whereas the areas where abundances are predicted to be high are estimated to be relatively stable (Figure 3b-c). The fall year-to-year coefficient of variation is estimated to vary across space such that there are areas with high abundance that are relatively stable and others that vary from year-to-year (Figure 3b-c). The standard error of the predictions is relatively consistent across the region but is higher at the boundaries of the prediction extent and in between Texada and Lasqueti Islands (Figure 3d), where the survey does not fish (Figure 1).

3.2 Coho Salmon

Our model estimates that juvenile Coho Salmon are present only in the surface 45 m (headrope depth 0 and 15, and 30 m; Figure A.2c). Juvenile Coho Salmon were caught in 79.5% of sets in this depth range. A total of 42,102 individuals was caught across all surveys, which equals 23.6% of all individuals caught across all species. In early summer, juvenile Coho Salmon are predicted to be most abundant in the central and northeastern part of the Strait of Georgia and least abundant near the Fraser River outflow (Figure 4a). In fall, this gradient is predicted to intensify, with high abundances predicted in the northeastern part of the strait. In both seasons, these areas of high predicted abundance in the central and northeastern part of the Strait of Georgia are estimated to be relatively stable across years (i.e., low temporal CV; Figure 4b-c). We estimate high temporal variability in abundances across years in both seasons in the low abundance area of the southwest basin of the strait, near Howe Sound and the Fraser River outflow. The standard error of the predictions is relatively consistent across the region but is

higher at the boundaries of the prediction extent and in between Texada and Lasqueti Islands (Figure 4d), where the survey does not fish (Figure 1).

3.3 Pink Salmon

Our model estimates that juvenile Pink Salmon are present in the surface 30 m (headrope depth 0 and 15 m; Figure A.2d). Juvenile Pink Salmon were caught in 67.7% of sets in this depth range in even years. A total of 42,715 individuals was caught across all surveys, which equals 23.9% of all individuals caught across all species. In summer, juvenile Pink Salmon are predicted to be most abundant in the northeastern part of the Strait of Georgia, although abundances are predicted to be relatively high in all parts of the region except for near the Fraser River outflow (Figure 5a). This distribution is predicted to remain relatively consistent into the fall, although abundances are predicted to be lower on average. The temporal CV in summer is estimated to be high across the central and southern portions of the Strait of Georgia, but lower in the northern part of the strait (Figure 5b). As a result, juvenile Pink Salmon are predicted to be consistently abundant in summer in the northern Strait of Georgia, but variably abundant in the central portion of the strait (Figure 5c). In fall, the most consistent areas of high abundance are in the northern portion of the strait. The standard error of the predictions is relatively consistent across the region but is higher at the boundaries of the prediction extent, particularly near the Fraser River outflow (Figure 5d).

3.4 Sockeye Salmon

Our model estimates that juvenile Sockeye Salmon are present in the surface 30 m (headrope depth of 0 and 15 m; Figure A.2e). Juvenile Sockeye Salmon were caught in 40% of sets in this depth range. A total of 7,673 individuals was caught across all surveys, which equals 4.3% of all individuals caught across all species. In summer, juvenile Sockeye Salmon are predicted to vary across the region with the lowest abundance in the southwest part of the region and the highest abundance in the northeastern part of the Strait of Georgia near the Discovery Islands (Figure 6a). In fall, this distribution is predicted to shift entirely so that the highest abundance is in the region near the entrance to Howe Sound and along the Sunshine Coast. In summer, the areas with the highest predicted abundance are estimated to vary moderately across years (i.e., medium temporal CV; Figure 6b,c), whereas the high abundance areas in fall are estimated to be relatively consistent across years. Sockeye Salmon have the highest estimated year-to-year variation in CPUE across all of the species (Figure 6b). The standard error of the predictions is relatively consistent across the region but is higher at the boundaries of the prediction extent and in between Texada and Lasqueti Islands (Figure 6d), where the survey does not fish (Figure 1).

4 Discussion

This analysis illustrates that all of the Strait of Georgia is habitat for juvenile Pacific salmon as illustrated by the estimated spatial distributions of the species, as well as the fact that Pacific salmon were caught in almost all (94.8%) survey sets, particularly those targeting 0 and 15 m depths (97.6%). However, there is notable variation in the distributions across species and across seasons. Despite year-to-year variation, both in mean abundances and in the distribution patterns, our models estimate that there are areas in the region where abundances are consistently high or low within each season, across years. However, there are also areas that show high year-to-year variability in abundance.

4.1 Chinook Salmon

The distributional shift in the juvenile Chinook Salmon between the summer and fall surveys that was identified in the model output can be explained by a shift in the stock structure between these surveys (Beamish et al. 2010, 2013). Most Chinook Salmon enter the strait in the late spring (~May) and these fish are caught in the June survey. However, Chinook Salmon from the South Thompson watershed on the Fraser River (age 0.x) enter the strait six to eight weeks later (late June - early July). In the September survey, these South Thompson Chinook Salmon represent from 50 to 70% of the juvenile Chinook Salmon caught in the survey. The numbers of the earlier ocean entrants are reduced in number due to a combination of early marine mortality and migration and also based on life history type (Beamish et al. 2011; Neville et al. 2015).

4.2 Chum Salmon

Chum Salmon have the highest catch numbers (31.3%) of all juvenile Pacific salmon (other than Pink Salmon in some years). Our results show this species uses all of the strait and are caught across all regions in both seasons. They remain one of the dominant species of Pacific salmon in the September surveys. Current research by the Salmon Marine Interactions Program is examining the stock structure of the juveniles across this time period to determine if there is stock specific residency within the strait.

4.3 Coho Salmon

The model outputs for Coho Salmon distributions are what would be expected based on current knowledge of this species. Chittenden et al. (2009) demonstrated that most juvenile Coho Salmon enter the Strait of Georgia in early spring and they remain and rear in this region until October–November of their first ocean year. Therefore, the stock mixture between the summer and fall surveys remains relatively consistent. Neville and Beamish (2018) report increased concentrations of Coho Salmon in the northern portion of the strait during the September surveys.

Beamish and Neville (2021), however, report that there are abrupt shifts in productivity that occur for Coho Salmon in the strait as well as changes in overwinter behaviour. They discuss the change that occurred in the 1990s when virtually all Coho Salmon left the strait and did not return until the late summer of their second marine year. Although a proportion of the Coho Salmon originating from this region had always migrated out of the strait, this shift to virtually all Coho Salmon moving out was unprecedented according to their report, and in combination with declining marine survivals resulted in the closure of fisheries in this region. Beamish and Neville (2021) also report a more recent shift in productivity occurring about 2009 when the September surveys observed an increase in both CPUE and in the average size of the juveniles. This shift appears to also be associated with a change in distribution as they report that in 2013 Coho Salmon were present in the strait in small numbers in the early summer and that overwintering was observed in 2017. Beamish and Neville (2021) suggest that the growth and condition of the juveniles was associated with this shift in distribution. Based on this hypothesis, the continued increased size and abundance of Coho Salmon in recent fall surveys (Neville 2023) would suggest that this overwintering behaviour has continued and there are large numbers of juvenile Coho Salmon currently overwintering in the strait, although the specific distribution of these fish within the strait is unknown.

4.4 Pink Salmon

Virtually all Pink Salmon in the strait originate from the Fraser River in even-numbered years and are expected to represent the majority of the Pink Salmon caught in the survey. Neville et al. (2016) report large numbers of Pink Salmon migrating north through the Discovery Islands in June. It is therefore likely that that the increased abundances observed in the northern strait by the model are reflecting this northward movement. However, there are also localized smaller populations of Pink Salmon in that region especially from populations on the east size of Vancouver Island (Quinsam River and Nile Creek) that may also be contributing to these model outputs.

4.5 Sockeye Salmon

The distribution predicted by the model for juvenile Sockeye Salmon in both the summer and fall surveys is supported by current published information on early marine distribution for this species (Preikshot et al. 2012, Neville et al. 2016). Most Sockeye Salmon in the strait originate from the Fraser River and enter the ocean in April–May as age 1.x fish (one freshwater winter; Neville et al. 2016). Preikshot et al. (2012) estimated that by early July, more than 90% of these juveniles would have left the strait with peak abundance mid-June. Neville et al. (2016) showed that most of the migration of these juveniles was northward through Johnstone Strait with peak migration occurring in late May or early June. They also demonstrated that the juveniles accumulated in the northern portion of the strait prior to moving through the southern Johnstone Strait region over a very short period of time (weeks). The model outputs effectively show this northerly distribution of these juveniles in the summer survey (Figure 6), even though these surveys occur after the peak migration. The higher year-to-year coefficient of variation in the model outputs for Sockeye Salmon can be explained by the strong four-year pattern of returns of Fraser River Sockeye Salmon with both dominant and non dominant run cycles.

The southward distribution of juvenile Sockeye Salmon demonstrated in the model outputs of the September surveys reflects the influx of a different life history type of Sockeye Salmon (ocean type) that enter the ocean in the year they emerge (age 0.x, Gilbert, 1914). Beamish et al. (2013) report that in the strait, these ocean type Sockeye Salmon are from the Harrison River and represent the majority of the juvenile Sockeye Salmon caught at this time. They indicate that these Harrison River fish initially rear primarily in Howe Sound (outside of sets in our model) but continue to be concentrated in the southeastern strait in September.

4.6 Uncertainty

Although the models had relatively low uncertainty (Figures 1-5) and the estimated spatial patterns reflected the spatial and temporal variation in CPUE in the surveys (Figures A1-10), it is important to understand the limitations of these model predictions. Our model predictions represent the geometric mean CPUE and so are an average expectation, but do not reproduce the high inter-tow variability that is present in the survey data. Spatially, our predictions have low uncertainty in areas that are central within the standard survey track line (Beamish et al. 2000). However, uncertainty is higher on the margins of the survey area, where there are fewer sets to inform the model (Figure 1). The residuals for all of the models showed a reasonable fit to the data but were not perfect (Figure A.1). For most species, the observed CPUE was higher than the predicted CPUE at values in the middle of the range. However, these residuals are calculated only using the fixed effect predictions. Thus, it is possible that this deviation is

compensated for by the spatial and spatiotemporal random fields, which are not accounted for in the DHARMa package residuals (Hartig 2022).

4.7 Considerations

Our models are based on survey data from 2010 to 2020 and reflect distributions from this time period. Juvenile Pacific salmon abundances have undergone relatively abrupt shifts in abundance in the past and prior to this study period (e.g., Coho Salmon; Beamish and Neville 2021) that may be linked to shifts in the zooplankton (Perry et al. 2021) and the conditions regulating carrying capacity in the strait (Beamish and Neville 2021). Shifts in ocean climate, in addition to climate change is likely to lead to additional shifts in the future, and, without the underlying mechanisms regulating ocean survival identified for Pacific salmon species, it is unclear how this will affect the spatial distribution of juvenile Pacific salmon abundances in the strait. Detecting and assessing such shifts will require the continuation of fisheries independent surveys through the DFO Strait of Georgia juvenile salmon survey.

5 Conclusions

This analysis has documented that the entire Strait of Georgia is habitat for juvenile Pacific salmon during the period of June to October. There is variation in the abundance distributions across species and between summer (June–July) and fall (September–October) that may be related to ocean climate, stock distribution, or abundance. This analysis should provide a basis for incorporating juvenile Pacific salmon habitat use in the marine spatial planning processes that are currently underway in southern British Columbia as well as other scientific and management processes that would benefit from this knowledge.

6 Acknowledgements

We thank the captains and crews of the Canadian Coast Guard vessels *W.E. Ricker* and *Sir John Franklin* and of the charter commercial vessels *Nordic Pearl*, *Sea Crest* and *Frosti* for the completion of successful surveys. We also thank the numerous biologists and technicians that participated in the surveys or helped with the surveys' data. It is through their efforts that these surveys have been successful.

7 References

Anderson, S.C., Keppel, E.A., and Edwards, A.M. 2019. A reproducible data synopsis for over 100 species of British Columbia groundfish. DFO Can. Sci. Advis. Sec. Res. Doc. 041: vii + 321 p.

Anderson, S.C., Connors, B.M., English, P.A., Forrest, R.E., Haigh, R., and Holt, K.R. 2021. Trends in Pacific Canadian groundfish stock status. bioRxiv: 2021.12.13.472502.

Anderson, S.C., Ward, E.J., English, P.A., and Barnett, L.A.K. 2022. sdmTMB: An R package for fast, flexible, and user-friendly generalized linear mixed effects models with spatial and spatiotemporal random fields. bioRxiv 2022.03.24.485545.

Bakka, H., Vanhatalo, J., Illian, J.B., Simpson, D., and Rue, H. 2019. Nonstationary Gaussian models with physical barriers. Spatial Stat. 29: 268–288.

Beamish, R., and Neville, C.M. 2021. The Natural Regulation and Relevance of Wild and Hatchery Coho Salmon Production in the Strait of Georgia. Fisheries 46(11): 539–551.

Beamish, R.J., McCaughran, D., King, J.R., Sweeting, R.M., and McFarlane, G.A. 2000. Estimating the Abundance of Juvenile Coho Salmon in the Strait of Georgia by Means of Surface Trawls. North Am. J. Fish. Manage. 20(2): 369–375.

Beamish, R.J., Sweeting, R.M., Beacham, T.D., Lange, K.L., and Neville, C.M. 2010. A late ocean entry life history strategy improves the marine survival of chinook salmon in the Strait of Georgia. N. Pac. Anadr. Fish Comm. Res. Doc. 1282, 14 p. (available at www.npafc.org)

Beamish, R.J., Lange, K.L., Neville, C.M., Sweeting, R.M., and Beacham, T.D. 2011. Structural patterns in the distribution of ocean- and stream-type juvenile chinook salmon populations in the Strait of Georgia in 2010 during the critical early marine period. N. Pac. Anadr. Fish Comm. Res. Doc. 1354, 27 p. (available at www.npafc.org)

Beamish, R.J., Sweeting, R.M., and Neville, C.M. 2013. Late ocean entry timing provides resilience to populations of Chinook and sockeye salmon in the Fraser River. Technical Report, N. Pac. Anadr. Fish Comm. Tech. Rep. 9: 38–44. . (available at www.npafc.org)

Chittenden, C.M., Beamish, R.J., Neville, C.E., Sweeting, R.M., and McKinley, R.S. 2009. The Use of Acoustic Tags to Determine the Timing and Location of the Juvenile Coho Salmon Migration out of the Strait of Georgia, Canada. Trans. Am. Fish. Soc. 138(6): 1220–1225.

Cressie, N.A.C., and Wikle, C.K. 2011. Statistics for Spatio-Temporal Data. Wiley, Hoboken, N.J.

Currie, J.C., Thorson, J.T., Sink, K.J., Atkinson, L.J., Fairweather, T.P., and Winker, H. 2019. A novel approach to assess distribution trends from fisheries survey data. Fish. Res. 214: 98–109.

Diggon, S., Bones, J., Short, C.J., Smith, J.L., Dickinson, M., Wozniak, K., Topelko, K., and Pawluk, K.A. 2022. The Marine Plan Partnership for the North Pacific Coast – MaPP: A

collaborative and co-led marine planning process in British Columbia. Mar. Policy 142: 104065.

Ehler, C., and Douvere, F. 2009. Marine Spatial Planning: A step-by-step approach toward ecosystem-based management. Intergovernmental Oceanographic Commission and Man and the Biosphere Programme. UNESCO.

Gay, D.M. 1990. Usage Summary for Selected Optimization Routines. AT&T Bell Laboratories, Murray Hill, NJ 07974.

Hartig, F. 2022. DHARMa: Residual diagnostics for hierarchical (multi-level / mixed) regression models. manual.

Hilbe, J.M. 2011. Negative Binomial Regression. *In* 2nd edition. Cambridge University Press.

Kristensen, K., Nielsen, A., Berg, C.W., Skaug, H., and Bell, B.M. 2016. TMB: Automatic differentiation and laplace approximation. Journal of Statistical Software 70(5): 1–21.

Lindgren, F., and Rue, H. 2015. Bayesian spatial modelling with r-inla. J. Stat. Softw. 63(19): 1–25.

Lindgren, F., Rue, H., and Lindström, J. 2011. An explicit link between Gaussian fields and Gaussian Markov random fields: The stochastic partial differential equation approach: Link between Gaussian Fields and Gaussian Markov Random Fields. J. R. Stat. Soc. Ser. B (Stat. Meth.) 73(4): 423–498.

Neville, C. 2023. Juvenile salmon in the Strait of Georgia 2022. P. 224–227 *in* Boldt, J.L., Joyce, E., Tucker, S., and Gauthier, S. (Eds.). State of the physical, biological and selected fishery resources of Pacific Canadian marine ecosystems in 2022. Can. Tech. Rep. Fish. Aquat. Sci. 3542: viii + 312 p.

Neville, C.M., and Beamish, R.J. 2018. Understanding the Mechanisms that Regulate Coho Salmon Abundance in the Strait of Georgia, British Columbia, Canada. N. Pac. Andr. Fish Comm. Tech. Rep.11: 67–71.

Neville, C.M., Beamish, R.J., and Chittenden, C.M. 2015. Poor Survival of Acoustically-Tagged Juvenile Chinook Salmon in the Strait of Georgia, British Columbia, Canada. Trans. Am. Fish. Soc. 144(1): 25–33.

Neville, C.M., Johnson, S., Beacham, T., Whitehouse, T., Tadey, J., and Trudel, M. 2016. Initial Estimates from an Integrated Study Examining the Residence Period and Migration Timing of Juvenile Sockeye Salmon from the Fraser River through Coastal Waters of British Columbia. N. Pac. Anadr. Fish Comm. Bull. 6(1): 45–60.

Neville, C.M., Fitzpatrick, L.C., and Beamish, R.J. 2023. Juvenile Pacific salmon survey in the Strait of Georgia and associated waters, July 8-27, 2007. Can. Data Rep. Fish. Aquat. Sci. 1365: x + 378 p.

Olson, E.M., Allen, S.E., Do, V., Dunphy, M., and Ianson, D. 2020. Assessment of nutrient supply by a tidal jet in the northern strait of Georgia based on a biogeochemical model. J. Geophys. Res. Oceans 25(8).

Ovaskainen, O., and Abrego, N. 2020. Joint Species Distribution Modelling: With Applications in R. Cambridge University Press, Cambridge.

Pebesma, E. 2018. Simple Features for R: Standardized Support for Spatial Vector Data. R Journal 10(1): 439.

Perry, R.I., Young, K., Galbraith, M., Chandler, P., Velez-Espino, A., and Baillie, S. 2021. Zooplankton variability in the Strait of Georgia, Canada, and relationships with the marine survivals of Chinook and Coho salmon. PLoS ONE 16(1): e0245941.

PNCIMA. 2017. Pacific North Coast Integrated Management Area Area (PNCIMA) Initiative Management Area Plan: vii + 78 p. Available at 40743032.pdf (dfo-mpo.gc.ca)

Preikshot, D., Beamish, R.J., Sweeting, R.M., Neville, C.M., and Beacham, T.D. 2012. The Residence Time of Juvenile Fraser River Sockeye Salmon in the Strait of Georgia. Mar. Coast. Fish. 4(1): 438–449.

Robb, C.K., Fields, C., Agbayani, S., Greenberg, C., Huntington, S., and Guan, L. *in prep*. Spatial data to support marine spatial planning in the Pacific Region. Can. Tech. Rep. Fish. Aquat. Sci. XXXX: xx + xx p.

Rue, H., Martino, S., and Chopin, N. 2009. Approximate Bayesian inference for latent Gaussian models by using integrated nested Laplace approximations. J. R. Stat. Soc.: Ser. B (Stat. Meth.) 71(2): 319–392.

Sweeting, R.M., Beamish, R.J., Noakes, D.J., and Neville, C.M. 2003. Replacement of Wild Coho Salmon by Hatchery-Reared Coho Salmon in the Strait of Georgia over the past Three Decades. N. Am. J. Fish. Manage. 23(2): 492–502.

Thompson, P.L., Guzman, L.M., Meester, L.D., Horváth, Z., Ptacnik, R., Vanschoenwinkel, B., Viana, D.S., and Chase, J.M. 2020. A process-based metacommunity framework linking local and regional scale community ecology. Ecol. Lett. 23(9): 1314–1329.

Thorson, J.T., Shelton, A.O., Ward, E.J., and Skaug, H.J. 2015. Geostatistical delta-generalized linear mixed models improve precision for estimated abundance indices for West Coast groundfishes. ICES J. Mar. Sci. 72(5): 1297–1310.

Vehtari, A., Gelman, A., and Gabry, J. 2017. Practical Bayesian model evaluation using leave-one-out cross-validation and WAIC. Stat. Comput. 27(5): 1413–1432.

8 Figures

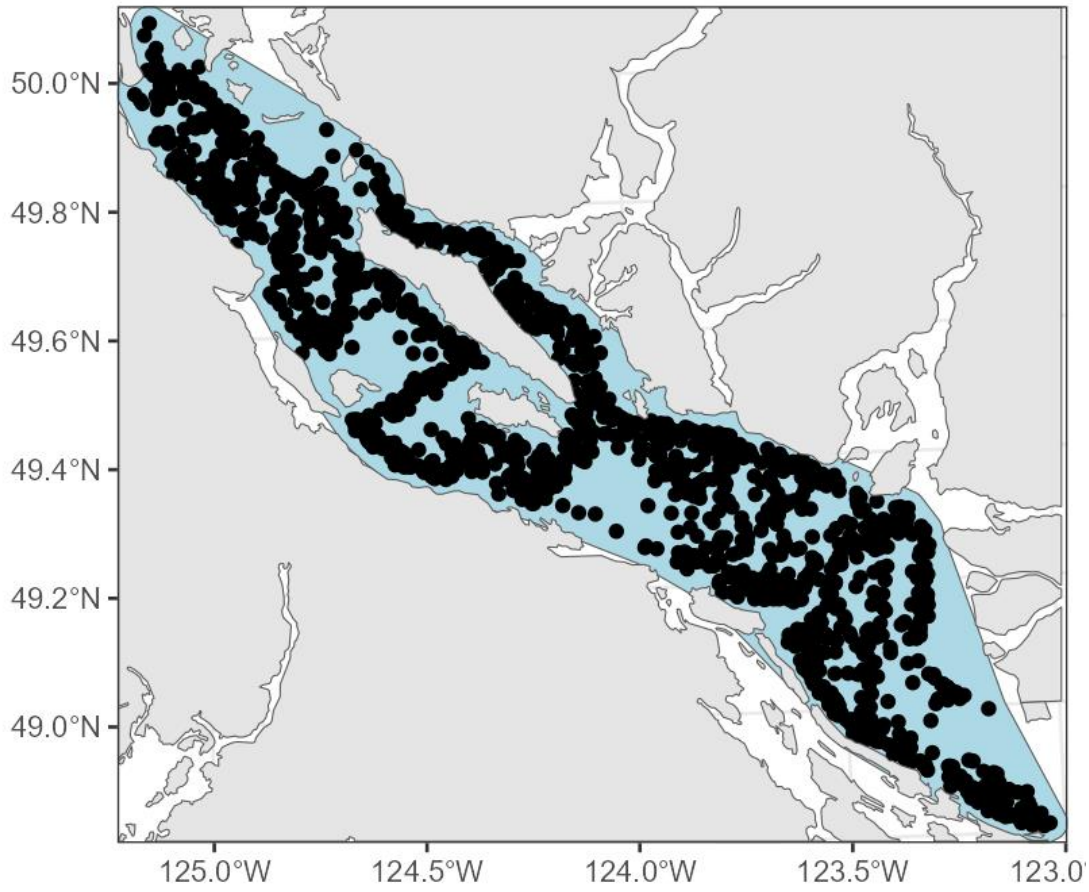

Figure 1. Map showing the location of the survey sets (black dots) and the 3 km buffered convex hull that defines the prediction extent.

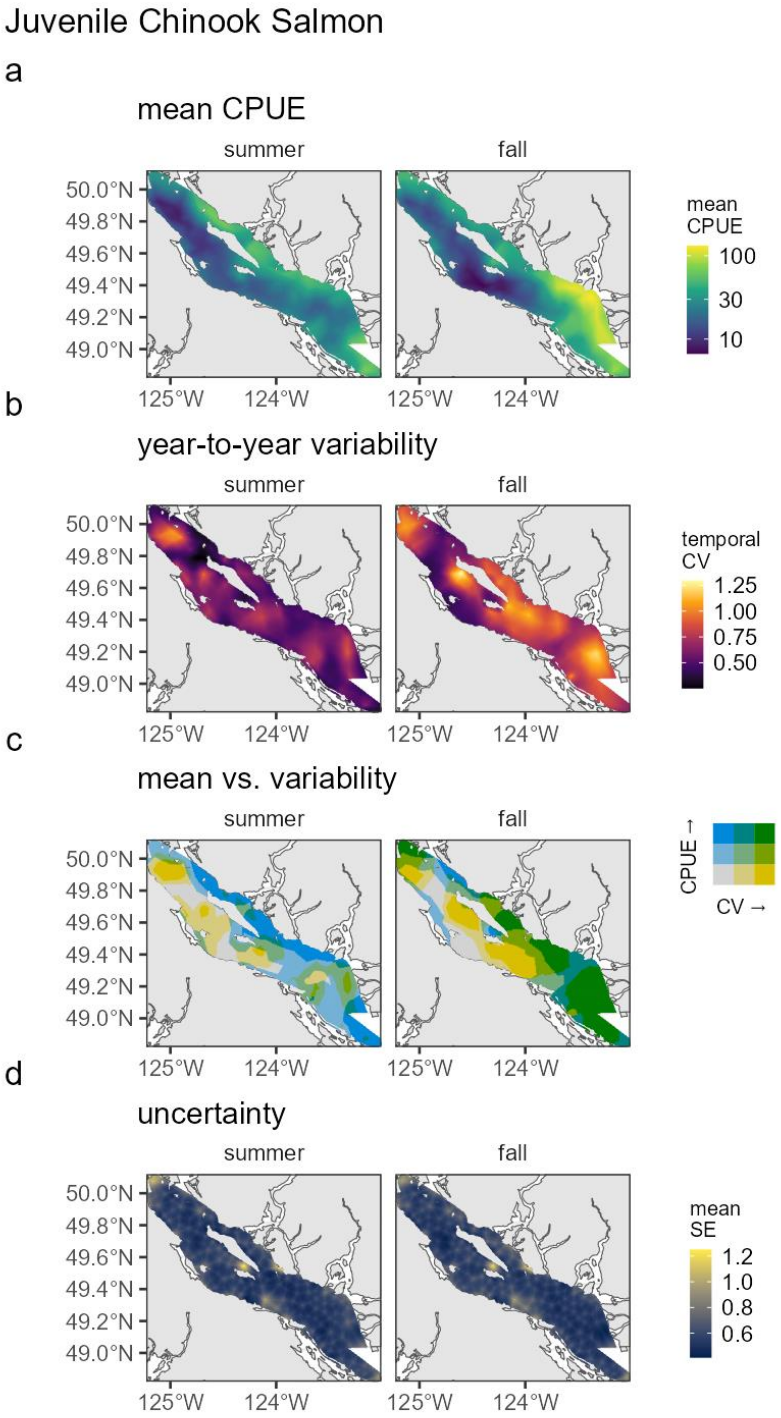

Figure 2. Predicted juvenile Chinook Salmon CPUE (catch per 60 min) in the summer (left) and fall (right) surveys. Panel a shows the mean across all years. Panel b shows the temporal coefficient of variation across all years to indicate year-to-year variation in estimated CPUE. Panel c shows mean CPUE vs. temporal CV on a bicolour scale to visually compare panels a and b. Panel d shows the mean standard error across all years, which represents the uncertainty in the estimates in panel a. The breaks in the colour scales in panel c are determined based on the 33rd and 66th quantiles of the data in panels a and b.

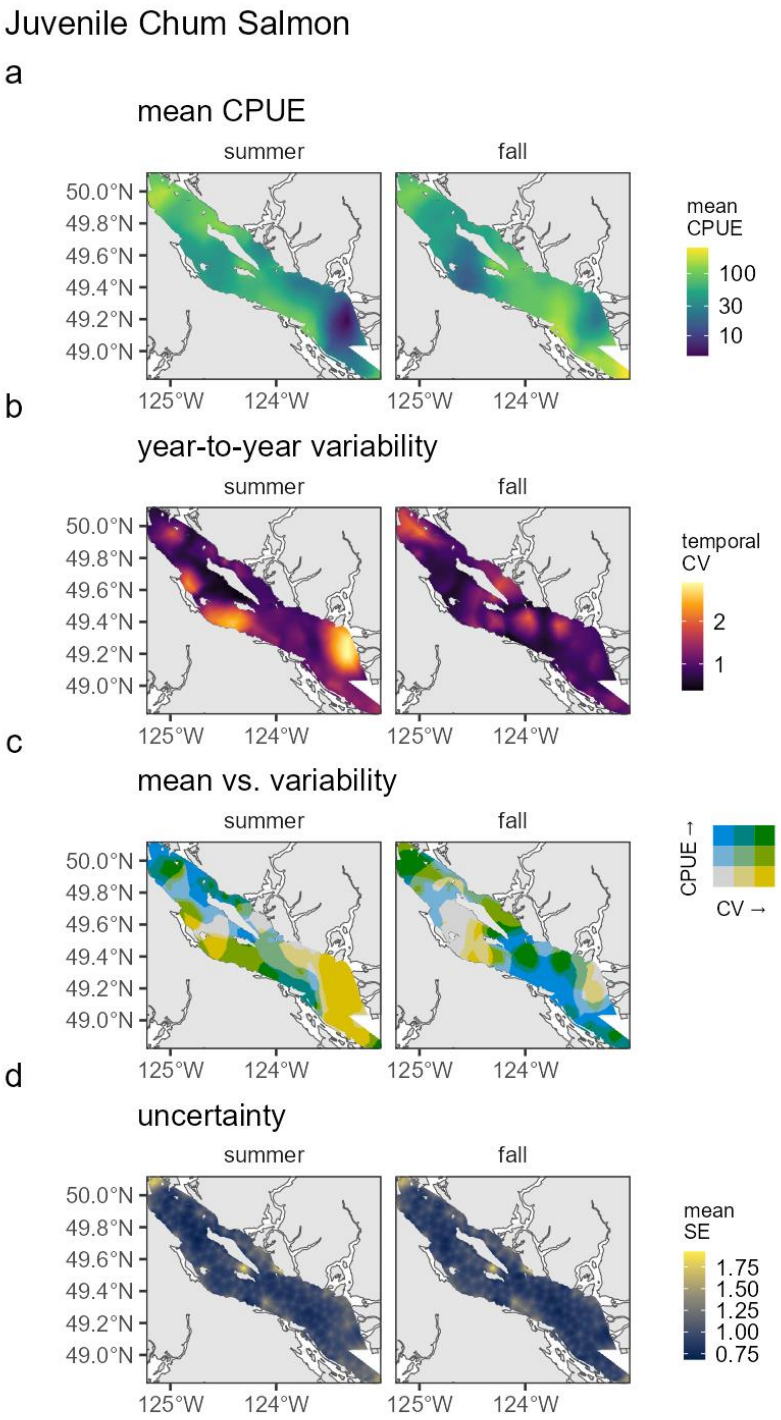

Figure 3. Predicted juvenile Chum Salmon CPUE (catch per 60 min) in the summer (left) and fall (right) surveys. Panel a shows the mean across all years. Panel b shows the temporal coefficient of variation across all years to indicate year-to-year variation in estimated CPUE. Panel c shows mean CPUE vs. temporal CV on a bicolour scale to visually compare panels a and b. Panel d shows the mean standard error across all years, which represents the uncertainty in the estimates in panel a. The breaks in the colour scales in panel c are determined based on the 33rd and 66th quantiles of the data in panels a and b.

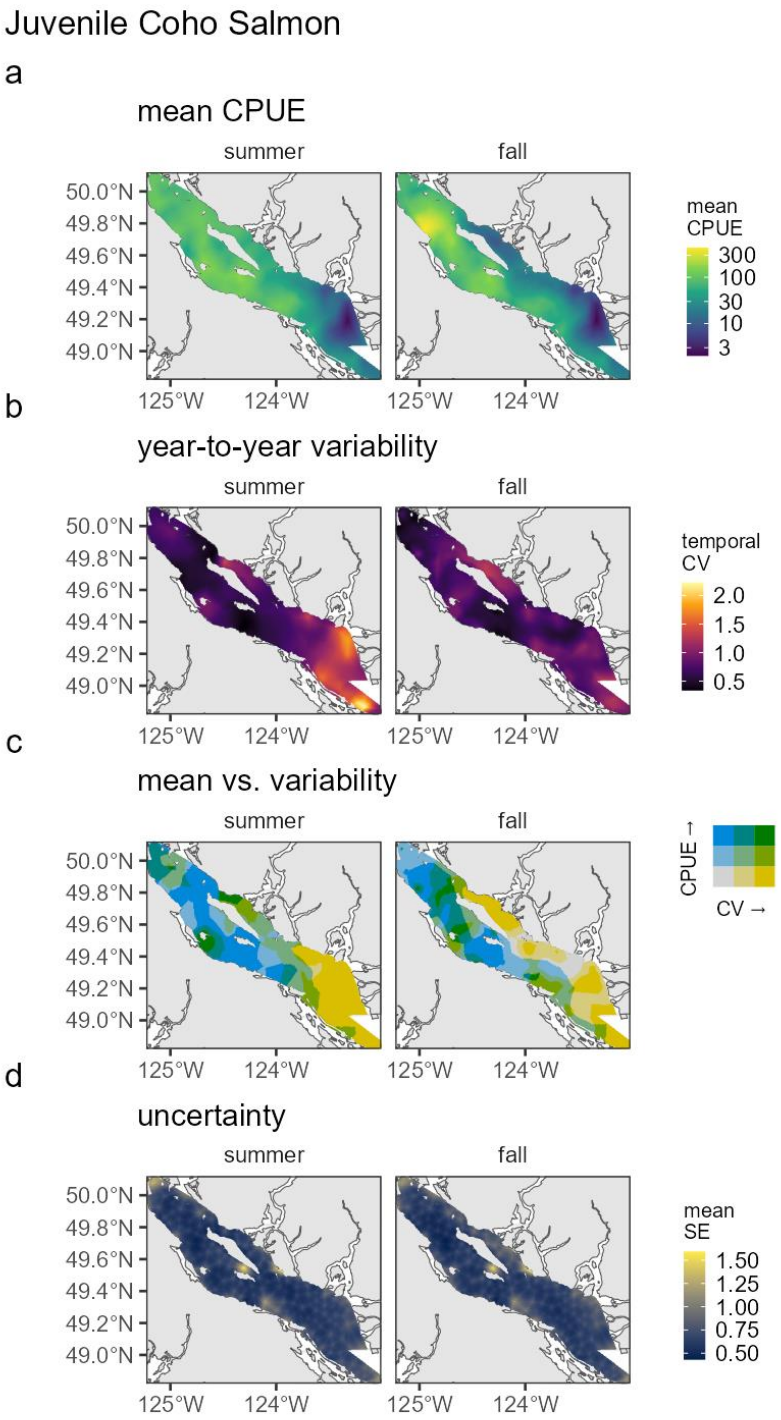

Figure 4. Predicted juvenile Coho Salmon CPUE (catch per 60 min) in the summer (left) and fall (right) surveys. Panel a shows the mean across all years. Panel b shows the temporal coefficient of variation across all years to indicate year-to-year variation in estimated CPUE. Panel c shows mean CPUE vs. temporal CV on a bicolour scale to visually compare panels a and b. Panel d shows the mean standard error across all years, which represents the uncertainty in the estimates in panel a. The breaks in the colour scales in panel c are determined based on the 33rd and 66th quantiles of the data in panels a and b.

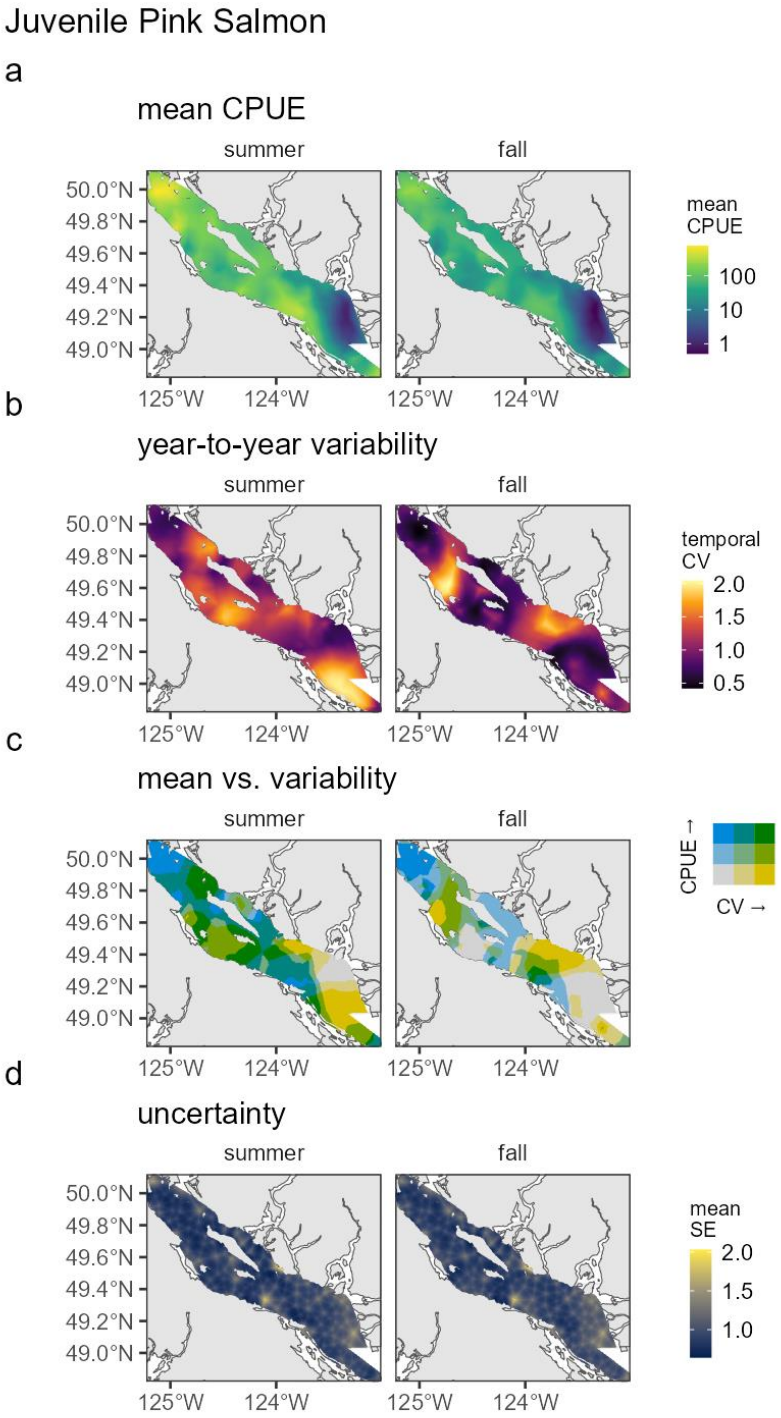

Figure 5. Predicted juvenile Pink Salmon CPUE (catch per 60 min) in the summer (left) and fall (right) surveys. Panel a shows the mean across all years. Panel b shows the temporal coefficient of variation across all years to indicate year-to-year variation in estimated CPUE. Panel c shows mean CPUE vs. temporal CV on a bicolour scale to visually compare panels a and b. Panel d shows the mean standard error across all years, which represents the uncertainty in the estimates in panel a. The breaks in the colour scales in panel c are determined based on the 33rd and 66th quantiles of the data in panels a and b.

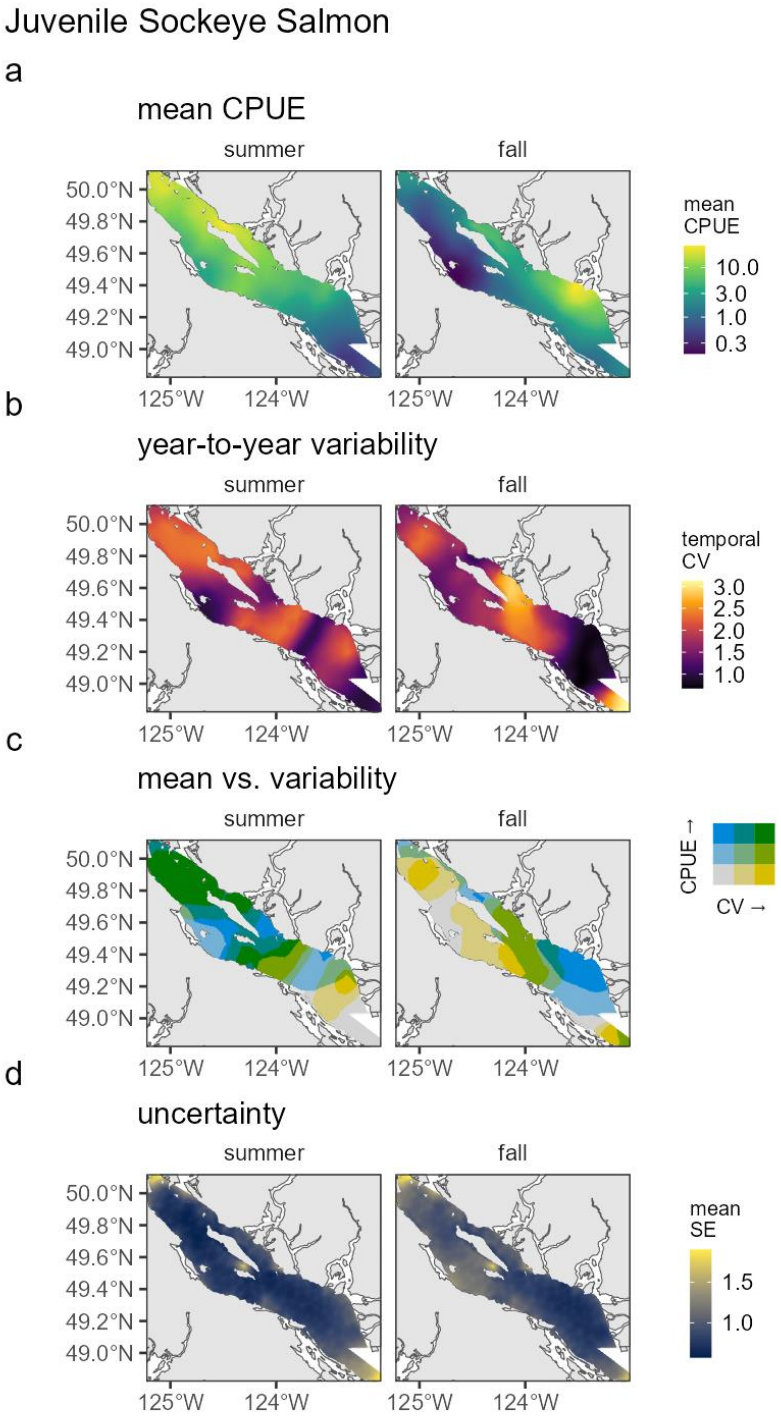

Figure 6. Predicted juvenile Sockeye Salmon CPUE (catch per 60 min.) in the summer (left) and fall (right) surveys. Panel a shows the mean across all years. Panel b shows the temporal coefficient of variation across all years to indicate year-to-year variation in estimated CPUE. Panel c shows mean CPUE vs. temporal CV on a bicolour scale to visually compare panels a and b. Panel d shows the mean standard error across all years, which represents the uncertainty in the estimates in panel a. The breaks in the colour scales in panel c are determined based on the 33rd and 66th quantiles of the data in panels a and b.

9 Appendix

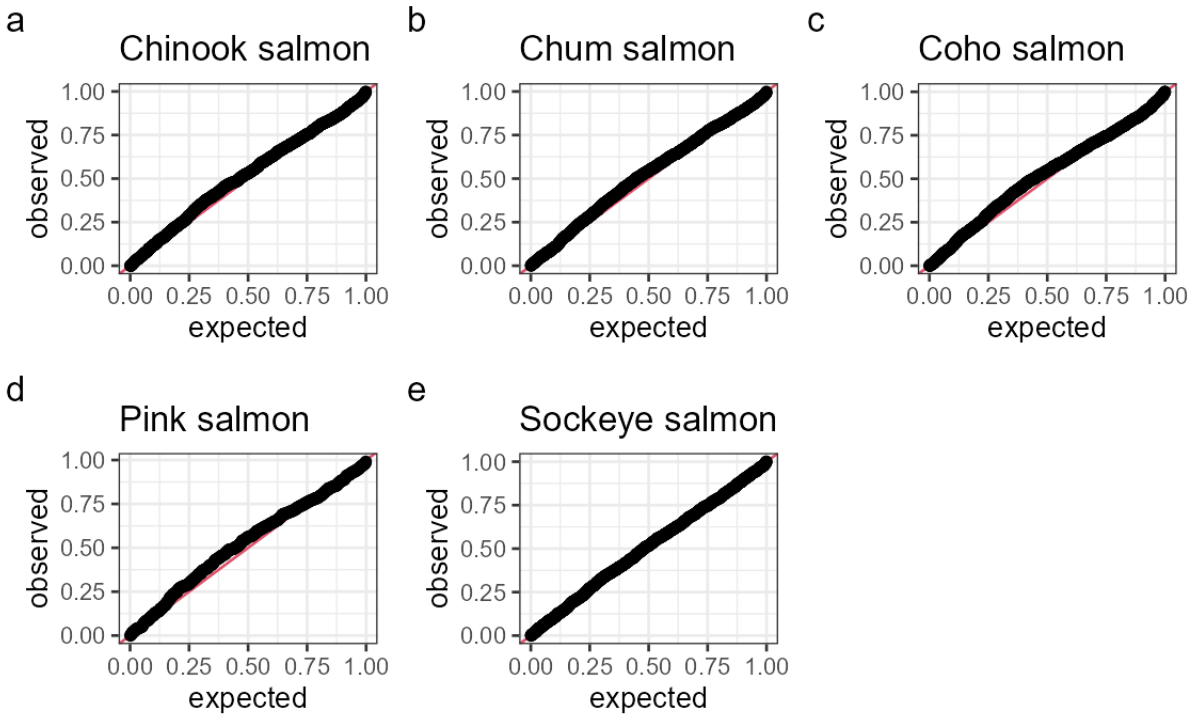

Figure A.1. Model residuals for the selected models, simulated using the DHARMa package (Hartig 2022). The red line indicates relationship if the expected and observed data were equal.

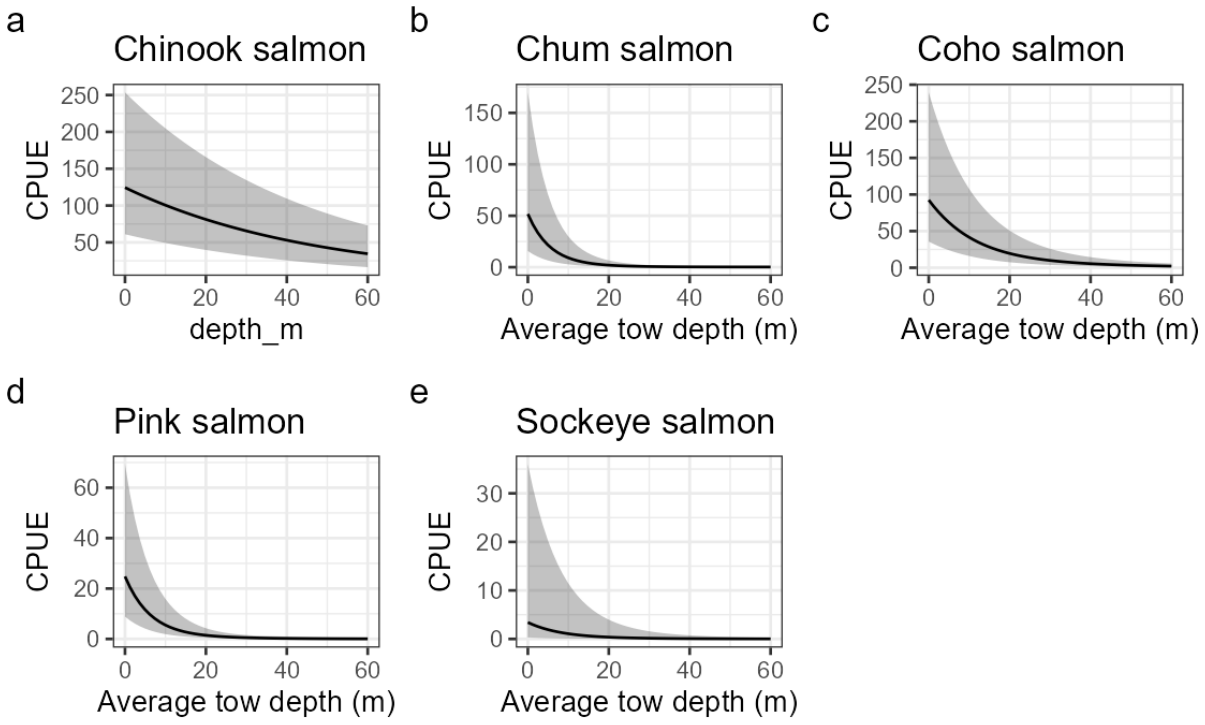

Figure A.2. Estimated CPUE (catch per 60 min) by headrope tow depth relationships for the five species. The lines represent the mean predicted CPUE and the shaded bands represent the 95 percent confidence interval.

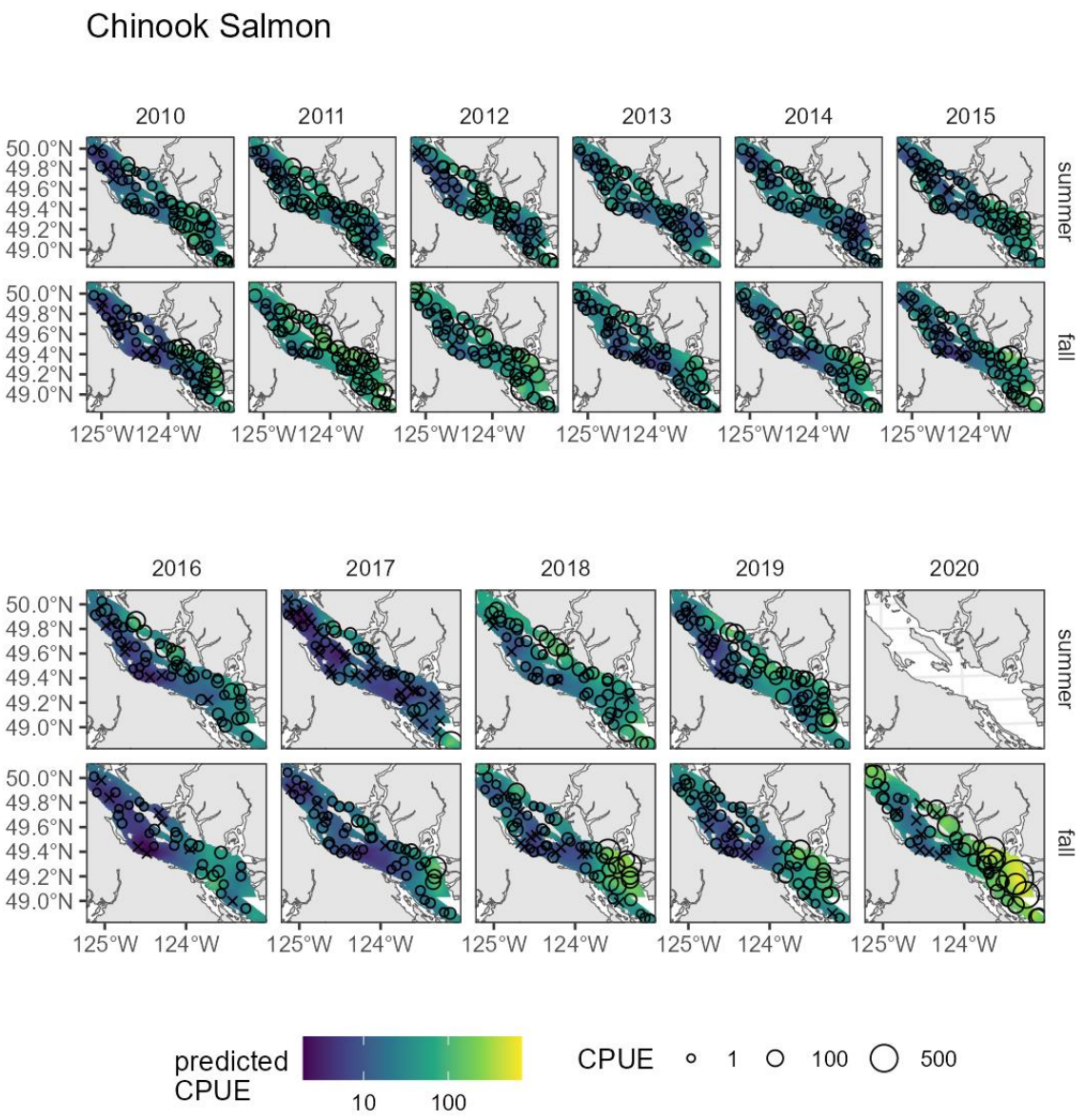

Figure A.3. Predicted juvenile Chinook Salmon CPUE (catch per 30 min) across years and seasons. The circles and crosses show the locations of the tows. Crosses mark tows where no juvenile Chinook Salmon were caught while the size of the circles indicates the CPUE of the catch. Predictions are for surface waters and so only data from depths shallower than 15 m are shown.

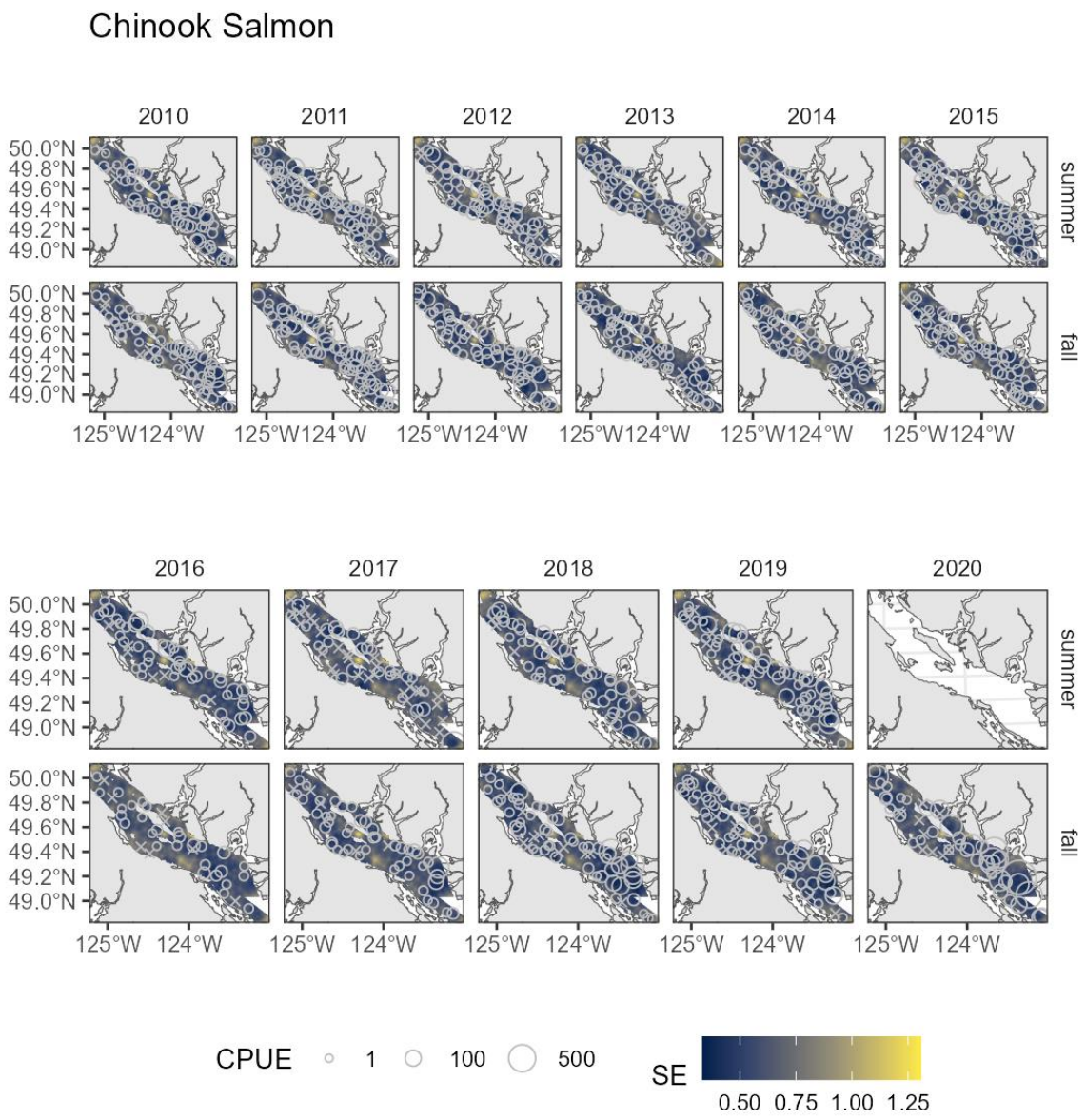

Figure A.4. Prediction standard error for juvenile Chinook Salmon CPUE (catch per 30 min) across years and seasons. The circles and crosses show the locations of the tows. Crosses mark tows where no juvenile Chinook were caught while the size of the circles indicates the CPUE of the catch. Predictions are for surface waters and so only data from depths shallower than 15 m are shown.

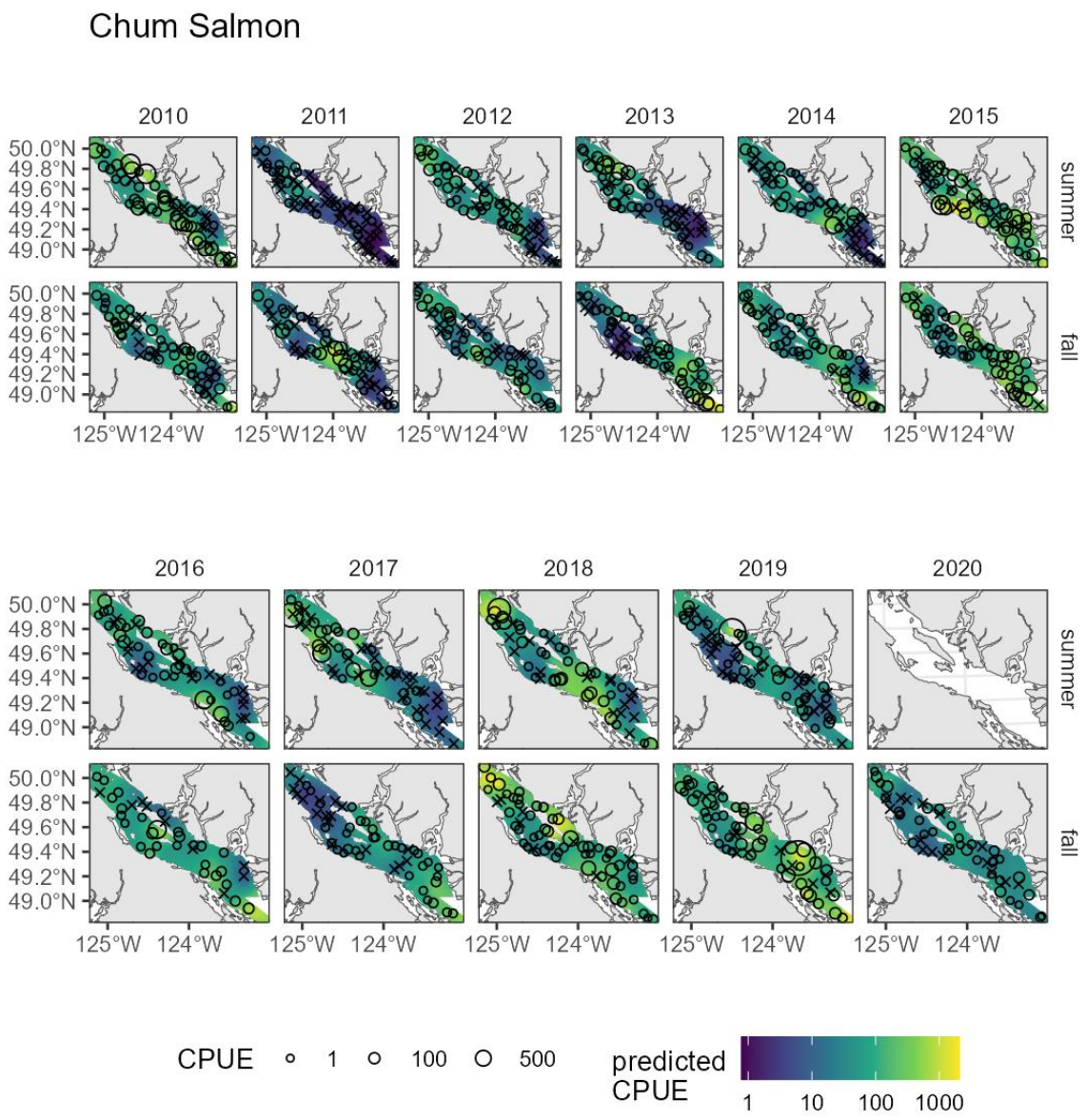

Figure A.5. Predicted juvenile Chum Salmon CPUE (catch per 30 min) across years and seasons. The circles and crosses show the locations of the tows. Crosses mark tows where no juvenile Chum were caught while the size of the circles indicates the CPUE of the catch. Predictions are for surface waters and so only data from depths shallower than 15 m are shown.

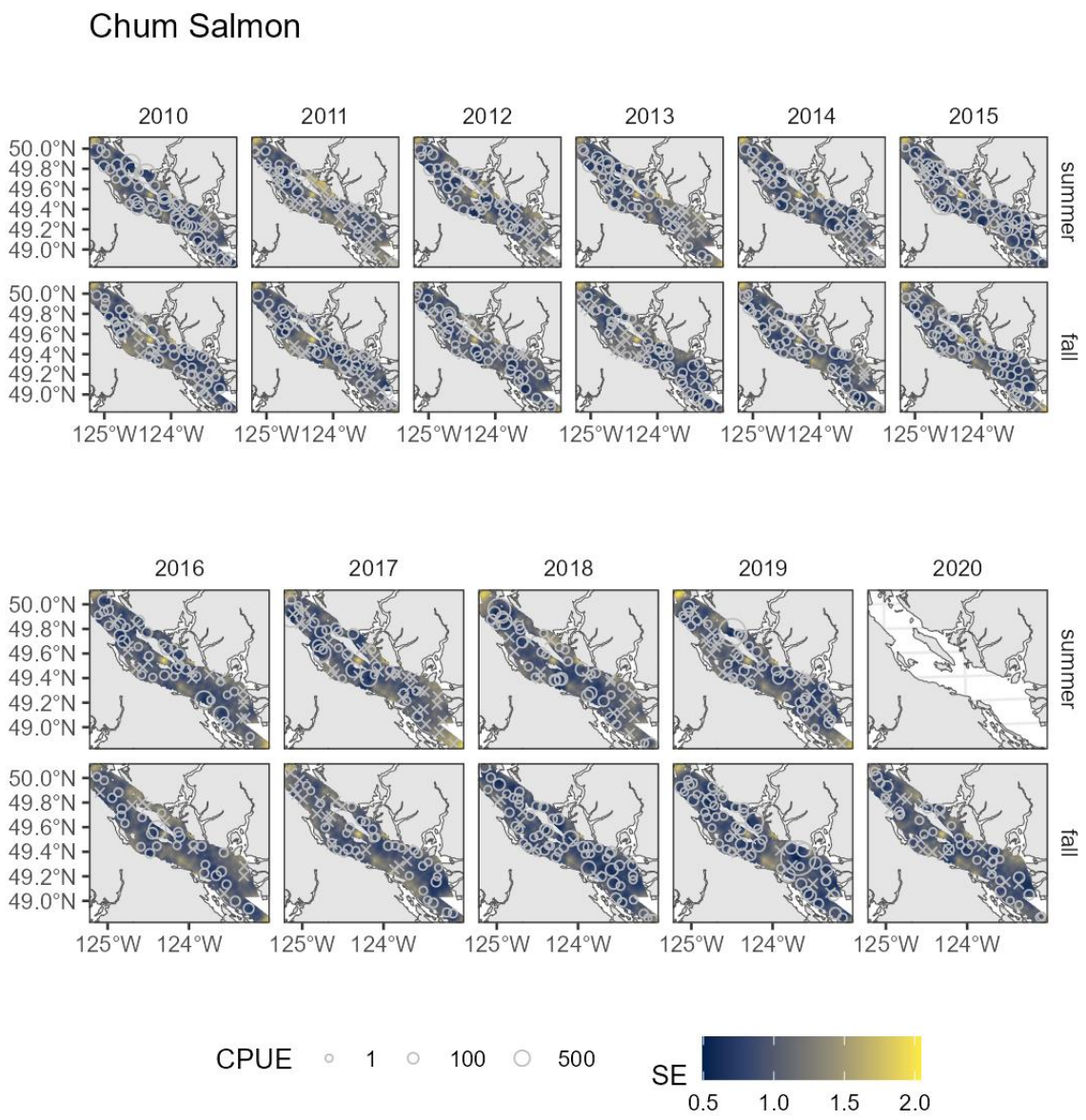

Figure A.6. Prediction standard error for juvenile Chum Salmon CPUE (catch per 30 min) across years and seasons. The circles and crosses show the locations of the tows. Crosses mark tows where no juvenile Chum were caught while the size of the circles indicates the CPUE of the catch. Predictions are for surface waters and so only data from depths shallower than 15 m are shown.

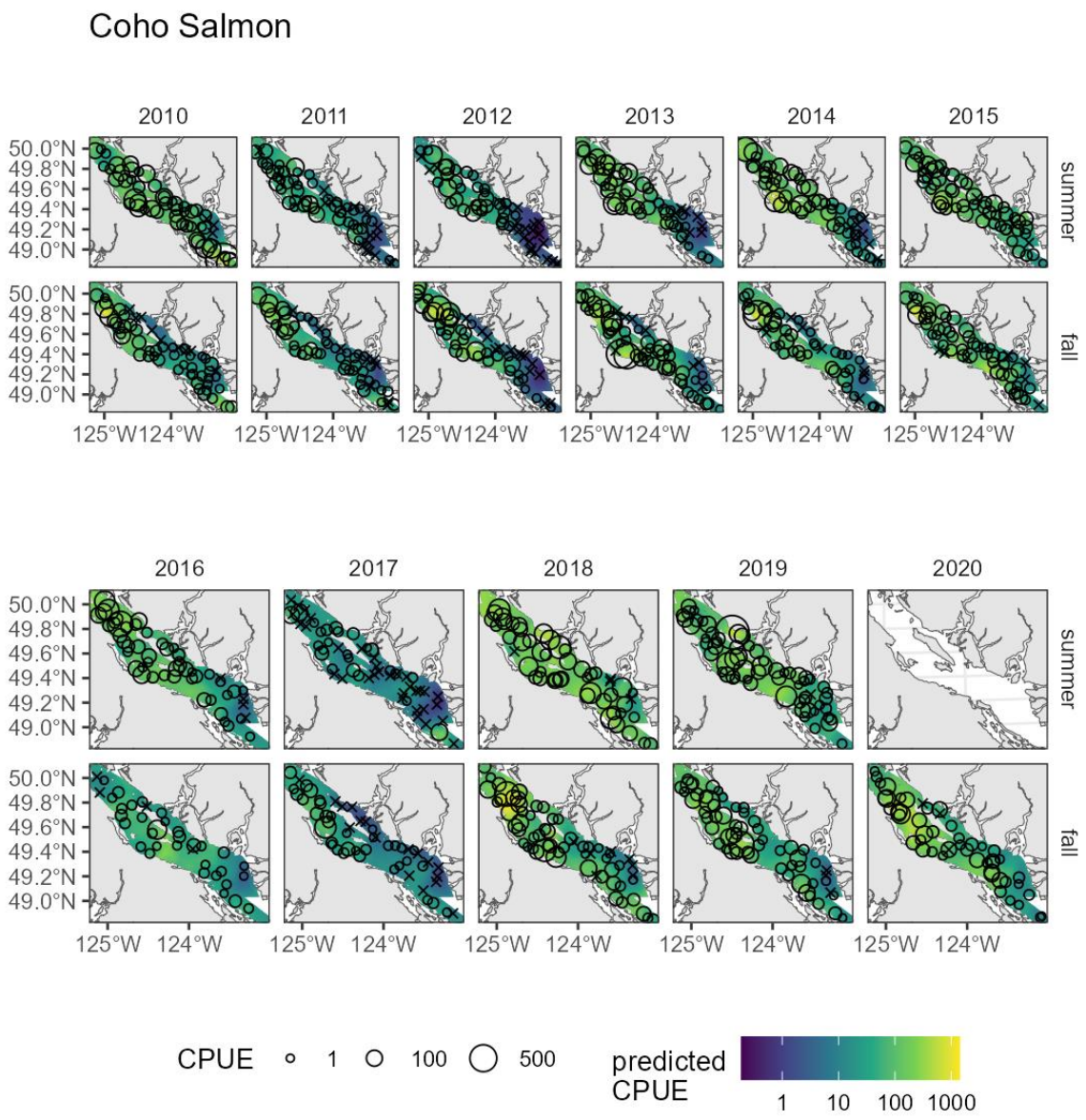

Figure A.7. Predicted juvenile Coho Salmon CPUE (catch per 30 min) across years and seasons. The circles and crosses show the locations of the tows. Crosses mark tows where no juvenile Coho were caught while the size of the circles indicates the CPUE of the catch. Predictions are for surface waters and so only data from depths shallower than 15 m are shown.

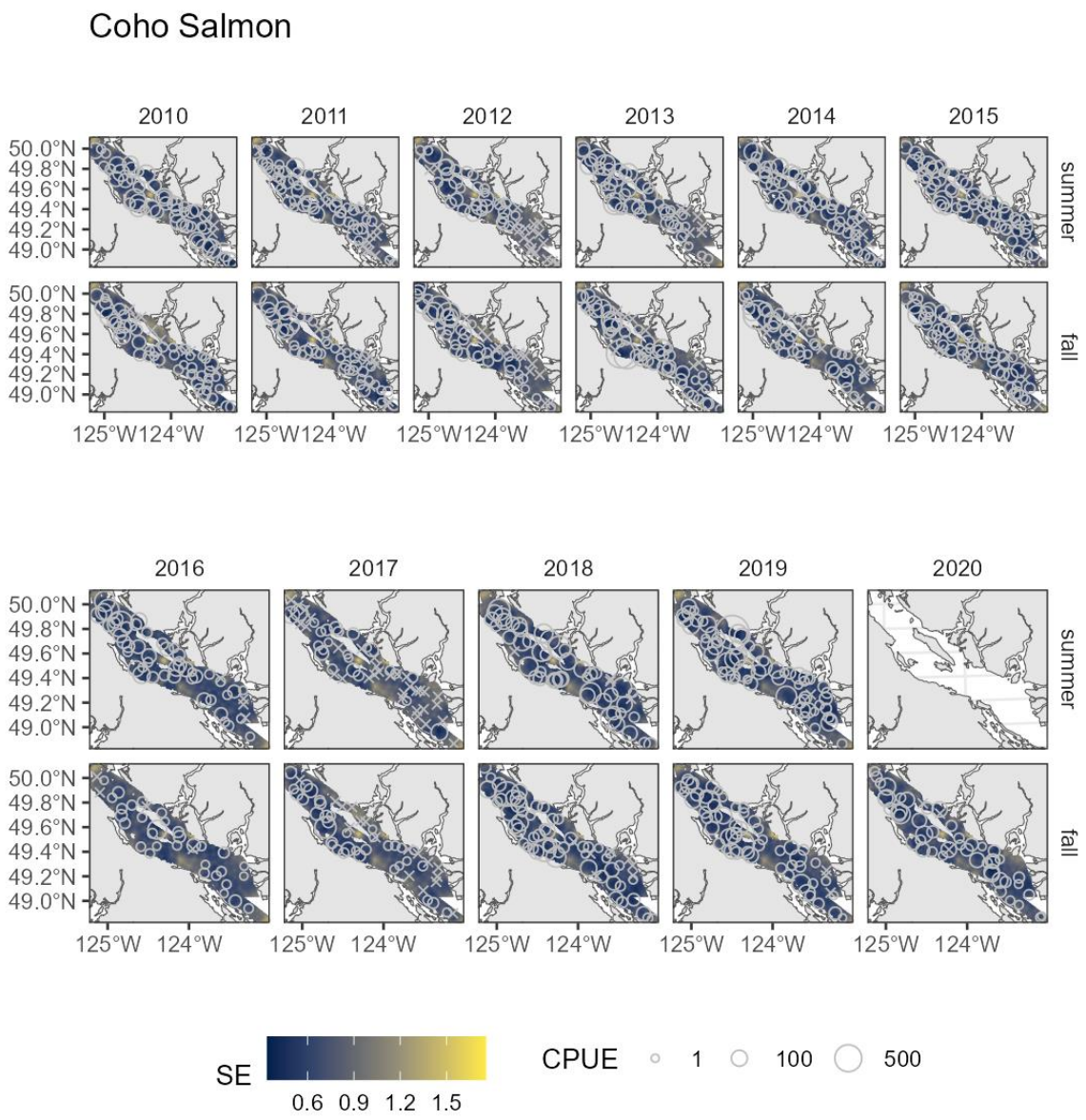

Figure A.8. Prediction standard error for juvenile Coho Salmon CPUE (catch per 30 min) across years and seasons. The circles and crosses show the locations of the tows. Crosses mark tows where no juvenile Coho were caught while the size of the circles indicates the CPUE of the catch. Predictions are for surface waters and so only data from depths shallower than 15 m are shown.

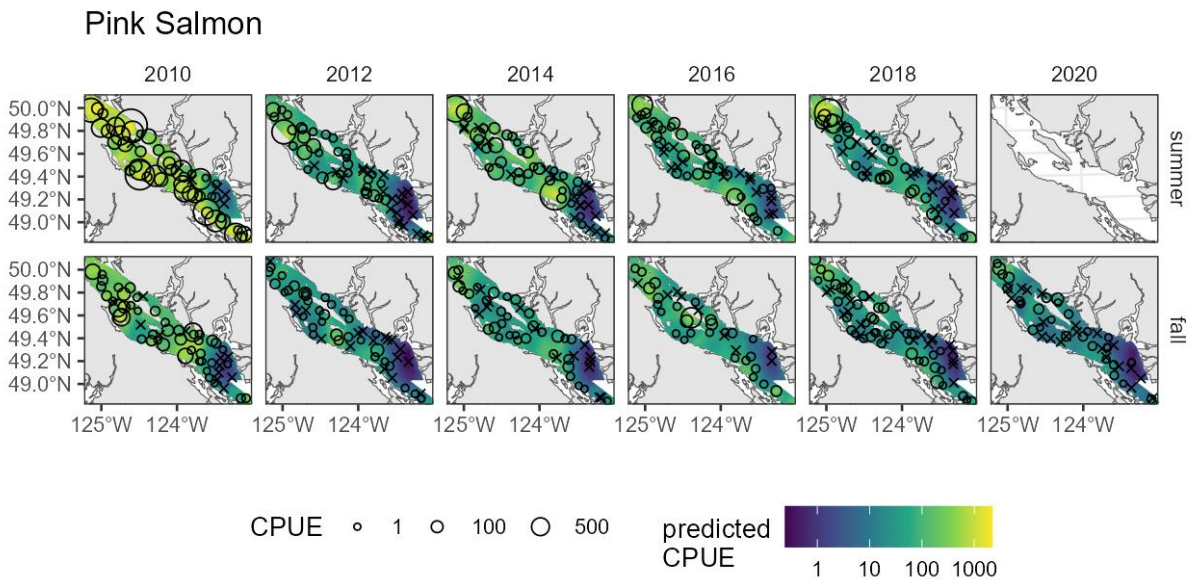

Figure A.9. Predicted juvenile Pink Salmon CPUE (catch per 30 min) across years and seasons. The circles and crosses show the locations of the tows. Crosses mark tows where no juvenile Pink were caught while the size of the circles indicates the CPUE of the catch. Predictions are for surface waters and so only data from depths shallower than 15 m are shown.

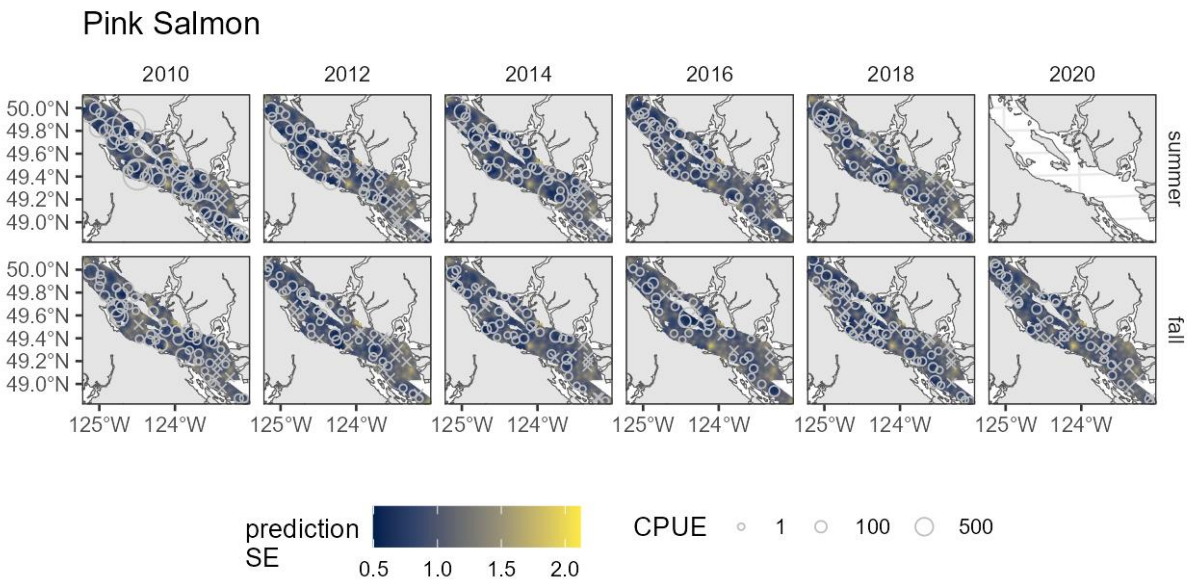

Figure A.10. Prediction standard error for juvenile Pink Salmon CPUE (catch per 30 min) across years and seasons. The circles and crosses show the locations of the tows. Crosses mark tows where no juvenile Pink were caught while the size of the circles indicates the CPUE of the catch. Predictions are for surface waters and so only data from depths shallower than 15 m are shown.

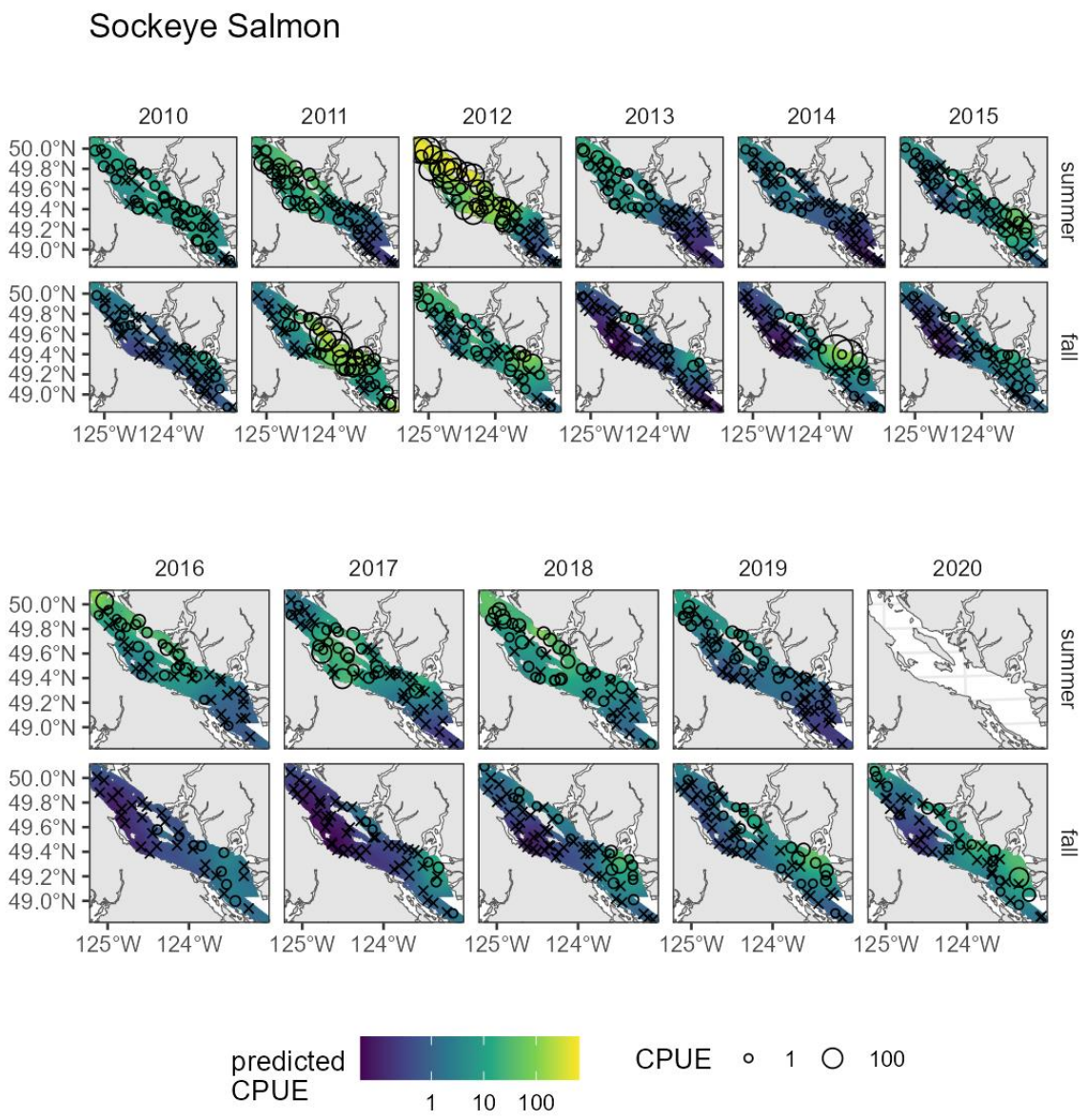

Figure A.11. Predicted juvenile Sockeye Salmon CPUE (catch per 30 min) across years and seasons. The circles and crosses show the locations of the tows. Crosses mark tows where no juvenile Sockeye were caught while the size of the circles indicates the CPUE of the catch. Predictions are for surface waters and so only data from depths shallower than 15 m are shown.

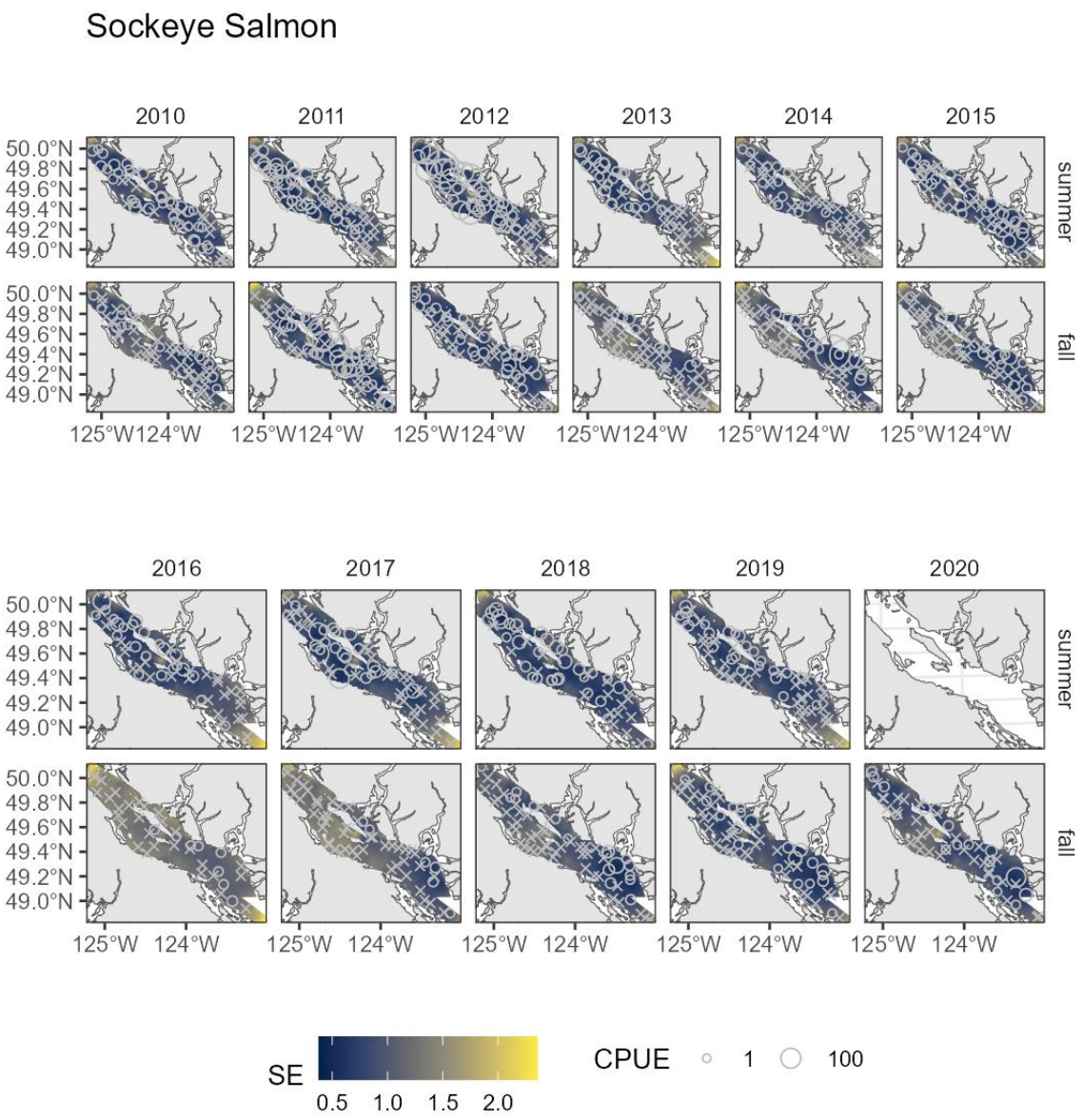

Figure A.12. Prediction standard error for juvenile Sockeye Salmon CPUE (catch per 30 min) across years and seasons. The circles and crosses show the locations of the tows. Crosses mark tows where no juvenile Sockeye were caught while the size of the circles indicates the CPUE of the catch. Predictions are for surface waters and so only data from depths shallower than 15 m are shown.